



Received: 12 September 2017

**Document 5-1/158-E
14 September 2017
English only****France****IMPACT OF IMT SYSTEMS ON TO INTER-SATELLITE SERVICE
IN 25.25-27.5 GHz****1 Introduction**

This document includes the sharing studies when IMT systems interfere with the inter-satellite service (ISS) in the 25.25-27.5 GHz frequency range and is intended to be responsive to part of *resolves to invite ITU-R 2 of Resolution 238 (WRC-15)* under WRC-19 agenda item 1.13.

2 Allocation information in the 25.25-27.5 GHz frequency range

The allocation of the inter-satellite service is provided in the following table extracted from the Radio Regulations:

TABLE 1
Frequencies allocation in Regions 1, 2 and 3 in 25.25-27.5 GHz

25.25-25.5	FIXED INTER-SATELLITE 5.536 MOBILE Standard frequency and time signal-satellite (Earth-to-space)
25.5-27	EARTH EXPLORATION-SATELLITE (space-to Earth) 5.536B FIXED INTER-SATELLITE 5.536 MOBILE SPACE RESEARCH (space-to-Earth) 5.536C Standard frequency and time signal-satellite (Earth-to-space) 5.536A
27-27.5 FIXED INTER-SATELLITE 5.536 MOBILE	27-27.5 FIXED FIXED-SATELLITE (Earth-to-space) INTER-SATELLITE 5.536 5.537 MOBILE

3 Technical characteristics

3.1 Technical and operational characteristics of IMT-2020 systems operating in the 25.25-27.5 GHz frequency range

3.1.1 Technical characteristics of IMT-2020 base station (BS) and user equipment (UE)

Table 2 provides the parameters related to BS and UE:

TABLE 2
BS and UE parameters

Parameter	Unit	BS	UE
Antenna array configuration $N_H \times N_V$	N/A	8×8	4×4
Single element output power	dBm/200 MHz	10	10
Maximum element gain	dBi	5	5
Conducted power ¹	dBm/200 MHz	28	22
Maximum composite antenna Gain	dBi	23	17
Array Ohmic losses	dB	3	3
Maximum e.i.r.p.	dBm/200 MHz	48	36
H/V ² radiating element spacing	N/A	$\lambda/2$	$\lambda/2$
Antenna height (above ground level)	m	6 (suburban hotspot, urban) 15 (suburban open space hotspot)	1.5 m (outdoor)
H/V ² 3 dB Beamwidth	°	65 for both	90 for both
Am and SLA	dB	30 for both	25 for both
Mechanical downtilt	°	10 (suburban hotspot, urban) suburban open space hotspot)	-90..90°

Moreover, as indicated in the previous TG 5/1 Chairman's Report (Document 5-1/92, Annex 1 section 11), sensitivity studies can be performed on the BS e.i.r.p. values in order to evaluate the impact on the results of the sharing analysis. Reminding that the Baseline study assumes 48 dBm e.i.r.p., two optional scenarios *up to 5 dB higher antenna element power* and 16×16 antenna array are carried out in this document.

3.1.2 Operational characteristics of IMT-2020 systems

3.1.2.1 Discussion on the calculation of the AAS gain with respect of the TRP assumption

Considering the response of Working Party 5D (Document [5-1/101](#)), for the purpose of sharing study, the *total radiated power (TRP)* of an IMT-2020 system can be understood as the summation inputs from the power amplifiers into each antenna element minus the losses within the AAS. Moreover Document 5-1/124 indicates the need to introduce a normalization factor to the calculation of the antenna directivity in each direction (using the formula in 3GPP TR 37.840 Table 5.4.4.2-3 and Rec. ITU-R M.2101 Table 4) in order to ensure that the total array directivity is equal to 0 dB.

¹ Without ohmic losses.

² Horizontal/Vertical.

Recalling the 3GPP expression for the composite array radiation pattern (TR 37.840):

$$\tilde{G}_{dB}(\theta, \varphi) = A_{E dB}(\theta, \varphi) + 10\log_{10} \left\{ 1 + \rho \left[\left| \sum_{m=1}^{N_H} \sum_{n=1}^{N_V} w_{m,n}(\theta, \varphi, \varphi_{scan}, \text{etilt}) v_{m,n}(\theta, \varphi, \varphi_{scan}, \text{etilt}) \right|^2 - 1 \right] \right\}$$

where:

$v_{m,n}$ called the ‘super position vector’ (see Rec. ITU-R M.2101 Section 5) can be understood as the steering vector giving the phase shift due to array placement;

$w_{m,n}$ depicts the weighting factor, is a function of the antenna beam pointing angles φ -scan and the electrical tilt and aims at tuning side lobe levels.

This actual array gain that has to be performed in any sharing studies should be normalised as follows:

$$D(\theta, \varphi, \varphi_{scan}, \text{etilt}) = \frac{\tilde{G}(\theta, \varphi, \varphi_{scan}, \text{etilt})}{\frac{1}{4\pi} \int_0^{2\pi} \int_0^{\pi} \tilde{G}(\theta, \varphi, \varphi_{scan}, \text{etilt}) \sin(\theta) d\theta d\varphi}$$

to ensure that $TRP = P_{Tx}$ where P_{Tx} is the conducted power input to the array system.

Consequently, this contribution accounts this normalization factor in the computation of the IMT-2020 systems antenna gain, i.e. BS and UE.

Finally, it has to be noted that the same document also indicates that 3GPP RAN4 confirmed that this normalization factor is correct.

3.1.2.2 Discussion on the calculation of the AAS gain with respect of the coordinate system

The IMT-2020 system antenna model is generally described and gain is calculated in a local coordinate system (BS and UE antenna own system). If the BS and UE antenna local coordinate system (the antenna of the IMT-2020 system) is oriented to be aligned with the global coordinate system (e.g., the Earth, azimuth = 0 and mechanical tilt = 0 (elevation = 90)), the two coordinate systems will be identical and the summation of power to all victims is straightforward.

But if the BS and UE are down tilted but still being aligned with global system in azimuth angle, a conversion of the antenna gain value in this GLS is needed before a summation is done (see Section 5.1.4 of 3GPP TS.36873). This has been done in this document.

3.1.2.3 BS deployment

The number of BS (N_{BS}) transmitting simultaneously within a land area of surface S is derived using the following formula:

$$N_{BS} = S \times BS_{AF} \times BS_{NLF} \times R_b \times (R_{aSU} \times (D_{BS_{SUO}} + D_{BS_{SU}}) + R_{aU} \times D_{BS_U})$$

with:

BS_{AF} the BS TDD activity factor (80%)³;

BS_{NLF} the BS network loading factor (20%)³;

R_a the ratio of hotspot areas to areas of cities/built areas/districts (3% for suburban (R_{aSU}) and 7% for urban (R_{aU}))³;

R_b the ratio built areas to total area of region in study (5%)³;

$D_{BS_{SUO}}$ BS density in the outdoor suburban open space (0 or 1 BS/km²)³;

³ See Document [5-1/36](#).

$D_{BS_{SU}}$ BS density in the outdoor suburban hotspot ($10 \text{ BS}/\text{km}^2$)³;

D_{BS_U} BS density in the outdoor urban hotspot ($30 \text{ BS}/\text{km}^2$)³.

The following analysis considers $D_{BS_{SU}} = 1$.

Finally, the computation of the BS and UE antenna gains requires the statistic of beam pointing orientation, i.e. electrical tilt and phi-scan angles because AAS are subject to time varying beam directions. Based on the TG 5/1 Chairman's Report (see Document 5-1/92, Annex 1, Section 12), it's also possible to perform the distribution of BS antenna beam pointing orientation angles (in e-tilt, φ-scan) towards UEs over the cell area by computing:

- the azimuth between UE and BS following a normal distribution $N(0^\circ, 30^\circ)$ with cutting off at $\pm 60^\circ$ angular sector. This angular sector contains 95% of the normally-distributed values resulting in 2.5% of the remaining tail-end values on either side;
- the distance (BS,UE) following
 - Rayleigh distribution with $\sigma = 32$ when UEs are connected to BS antenna height=6m above the ground,
 - Log-normal distribution with $\mu = 3.9$, $\sigma = 0.42$ when UEs are connected to BS antenna height=15 m above the ground.

3.1.2.4 UE deployment

The number of UEs (N_{UE}) transmitting simultaneously within a land area of surface S is derived using the following formula:

$$N_{UE} = S \times UE_{AF} \times UE_{NLF} \times R_b \times (R_{aSU} \times D_{UE_{SU}} + R_{aU} \times D_{UE_U})$$

with:

UE_{AF} the UE TDD activity factor (20%)³;

UE_{NLF} the network loading factor (20%)³;

R_a the ratio of hotspot areas to areas of cities/built areas/districts (3% for suburban (R_{aSU}) and 7% for urban (R_{aU}))³;

R_b the ratio built areas to total area of region in study (5%)³;

$D_{UE_{SU}}$ UEs density in the outdoor suburban ($30 \text{ UEs}/\text{km}^2$)³;

D_{UE_U} UEs density in the outdoor urban ($100 \text{ UEs}/\text{km}^2$)³.

The following analysis considers $D_{BS_{SU}} = 1$.

The statistic of the UE antenna beam pointing can be inherited from the BS, recalling that UE terminal points to the BS location in order to maximize the throughput of the link. However, the orientation of the device is of interest since this latter is influenced by the user behaviour (in addition to the beam steering) as depicted in the TG 5/1 Chairman's Report that the UE antenna panel positioning ("mechanical azimuth" and "mechanical tilt") "*has therefore to be considered randomly in elevation in the range -90 to 90° and in azimuth in the range -60° to +60° in the direction of the BS.*"

Another key parameter in the computation of the power radiated by UEs deals with the power control performed during the BS-UE radio link. The algorithm driving UE conducted power is taken from the Recommendation ITU-R M.2101 as follows (Section 4.2):

For IMT-Advanced systems, UE power control algorithm to be used in sharing studies is as follows:

$$P_{\text{PUSCH}}(i) = \min(P_{\text{CMAX}}, 10 \log_{10}(M_{\text{PUSCH}}(i)) + P_{0_{\text{PUSCH}}}(j) + \alpha(j) \cdot PL) \quad (23)$$

where:

- P_{PUSCH} transmit power of the terminal in dBm
 P_{CMAX} maximum transmit power in dBm
 M_{PUSCH} number of allocated RBs
 $P_{0_{\text{PUSCH}}}$ power per RB used target value in dBm
 α balancing factor for UEs with bad channel and UEs with good channel
 PL path loss in dB for the UE from its serving BS.

It is expected that for IMT-2020 systems UE power control algorithm could be similar to that used for IMT-Advanced networks.

It has to be noted that PL between UE and BS as defined in this Recommendation also covers other losses, i.e. body loss and (BS and UE) ohmic losses, if any but also the UE and BS antenna gains⁴ (respectively towards BS and UE). PL parameter can be understood as a coupling loss component. The input parameters required to derive the UE output power are extracted from Document 5-1/36 are provided in Table 3:

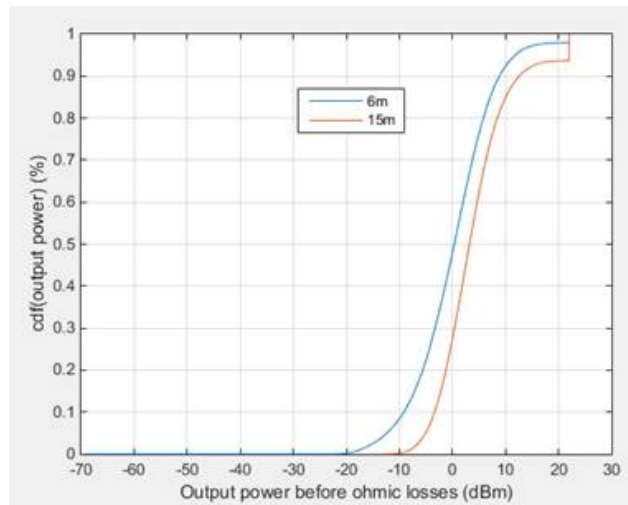
TABLE 3
UE Power control algorithm input parameters

Maximum user terminal output power P_{CMax}	dBm	22
Transmit power target value per $P_{0_{\text{PUSCH}}}$	dBm/180 kHz	-95
Pathloss compensation factor α	N/A	1
UE Body Loss	dB	4

Based on these parameters, the BS antenna beam pointing statistics, the distribution of the UE output power when connected to BS antenna at height = 6 m and 15 m was simulated as depicted by Figure 1. The curves show that a low percentage of UEs (<5%) is subject to transmit with maximum power P_{CMax} .

⁴ Calculated with the normalization factor.

FIGURE 1
UE conducted power distribution

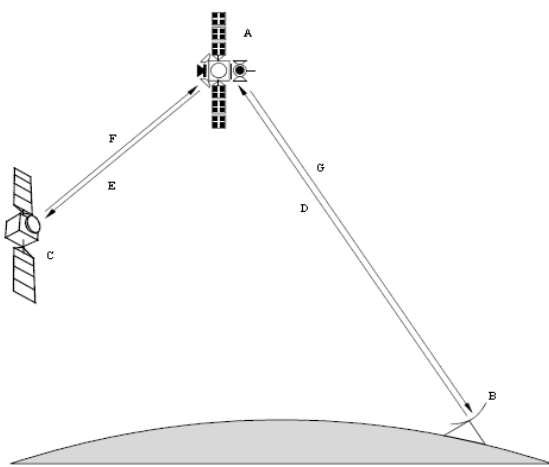


3.2 Technical and operational characteristics of ISS operating in the 25.25-27.5 GHz frequency range

3.2.1 Technical characteristics of ISS

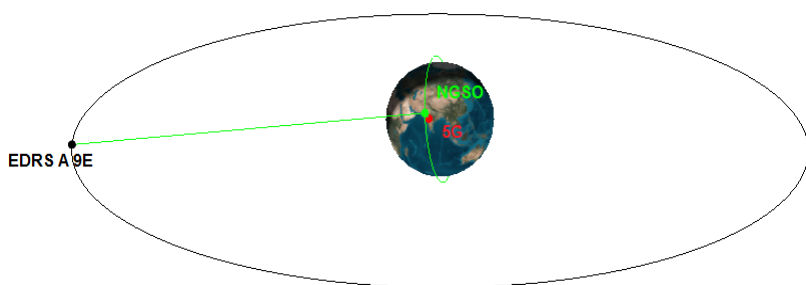
Figure 2 summarizes the different links used by the DRS systems. The band 25.25-27.25 GHz is a band for link **F** between non-GSO satellites (**C**) and the DRS satellite (**A**).

FIGURE 2
Different links used by DRS systems



The interference scenario is shown in Figure 3.

FIGURE 3
Interference scenario



Recommendation [ITU-R SA.1414-2](#) provides parameters for DRS systems worldwide to be used in interference sharing studies and Table 4 extracts the relevant parameters in the band 25.25-27.5 GHz.

TABLE 4
DRS ISL parameters

Network	Europe	Japan	United States of America	China	Russia
Orbital locations	Mainly low-Earth orbit				
Polarization	Circular				
Tx antenna gain (dBi)	≤ 50	≤ 49.7	≤ 47	≤ 44.5	≤ 46.1
Tx antenna radiation pattern	Rec. ITU-R S.672-4				
Receiving DRS					
Orbital locations	See Rec. ITU-R SA.1276				
Rx antenna gain (dBi)	49	58.8	55.9	57.5	57.4
Rx antenna radiation pattern	Rec. ITU-R S.672-4				
System noise temperature (K)	800	475	870	1 000	550

3.2.2 Protection criterion of ISS

Recommendation [ITU-R SA.1155-2](#) specifies the protection criteria for data relay satellite systems and presents them in the form of Io/No values. Concerning the 25.25-27.5 GHz, the protection criteria is defined as a maximum aggregate interference power spectral density (depicted in Table 5) to system noise power density ratio (Io/No), from all sources to be exceeded for no more than 0.1% of the time for the various links of data relay satellite systems is -10 dBs.

TABLE 5
DRS ISL protection criteria

Network	Europe	Japan	United States of America	China	Russia
Maximum Io dBW/Hz*	-209.6	-211.8	-209.2	-208.6	-211.2
Maximum Io dBm/Hz*	-179.6	-181.8	-179.2	-178.6	-181.2
* to be exceeded for no more than 0.1% of the time.					

3.2.3 Receiving DRS ISL satellite antenna pattern

Based on the TG 5/1 Chairman's Report (Document 5-1/92, Annex 1 Section 5), the gain to use in the sidelobes of the FSS space station antenna is the same as Recommendation ITU-R S.672-4 with $L_S^5 = -25$ dB. Since DRS GSO satellite has generally similar characteristics for the sidelobes as for FSS GSO satellite antenna operating with spot beams, $L_S = -25$ dB is also assumed for the ISS. Figure 4 shows the DRS satellite antenna gain versus off axis angle (see Rec. ITU-R S.672-4) for $L_S = -25$ dB and $z^6=1$.

FIGURE 4
DRS ISL satellite receiving antenna pattern

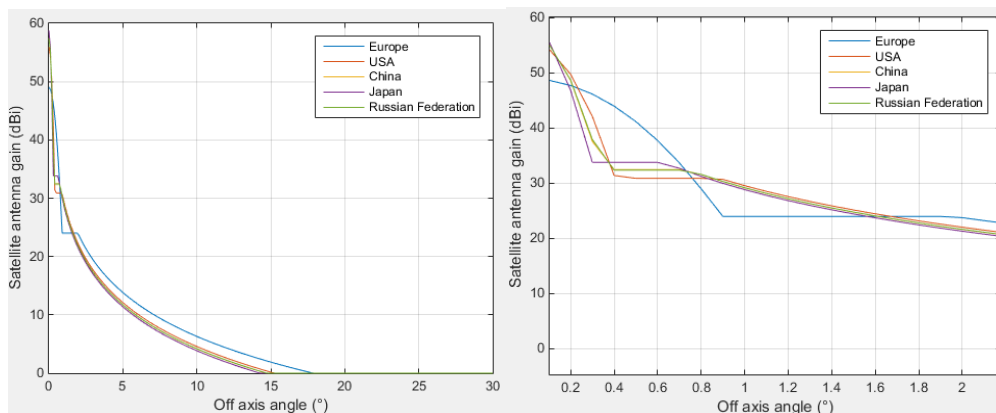


Figure 5 shows, as examples, the European DRS satellite (at 9°E) antenna gain over the Earth for 3 pointing directions (not at the same time):

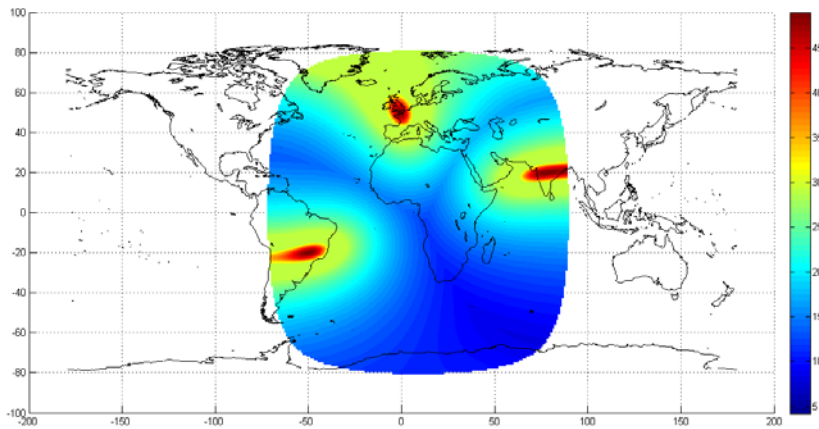
- toward the point on the Earth located at longitude -50° and latitude -20°.
- toward the point on the Earth located at longitude 78° and latitude 20°.
- toward the point on the Earth located at longitude -1° and latitude 50°.

⁵ L_S depicts the near-in-side-lobe level in dB relative to the peak gain required by the system design.

⁶ z represents the (major axis/minor axis) for the radiated beam.

FIGURE 5

Examples of European DRS antenna gain over the Earth



3.3 Propagation assumptions

Considered phenomena involved in the losses of the link budget between the GSO satellite and the IMT-2020 systems (BSs and UEs) are of different natures:

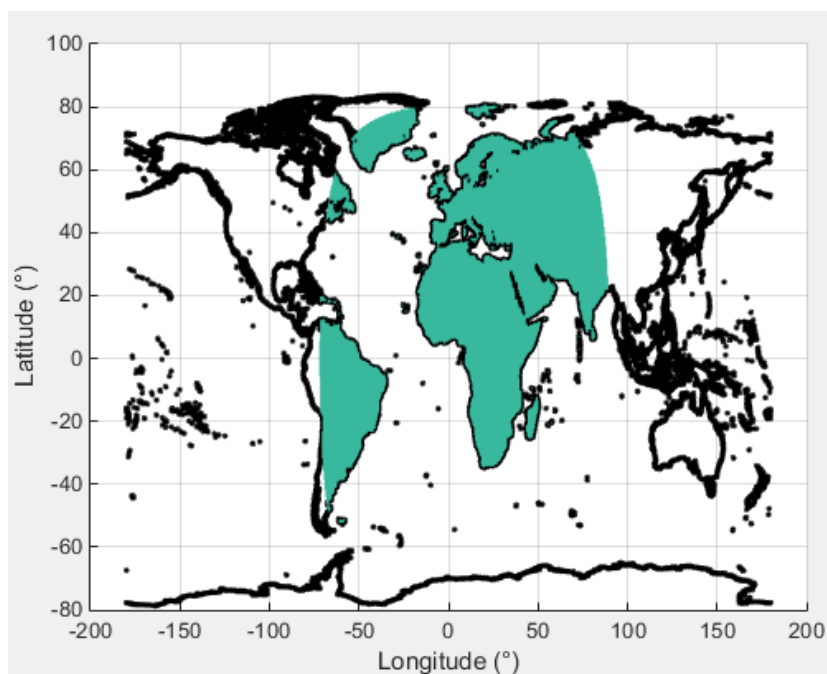
- the free space loss (using Rec. ITU-R P.525);
- loss due to atmospheric gases using Rec. ITU-R P.676-11, Annex 1 (Earth-space path);
- loss due to polarization: as outlined by the TG 5/1 Chairman's Report (Document 5-1/92, Annex 1 Section 9), aggregate studies should be *completed using both of the values of 0 dB and 3 dB for polarization discrimination*. Indeed, in case of cumulative effect of interference, coupling loss involves different range of antenna gain values (main lobe, sidelobes...) which makes the calculation of the discrimination in polarization necessary to account random elliptic polarization of the incident radio wave with respect of the receiving antenna. As analysed in Document [5-1/104](#), -3 dB (i.e., a loss of 3 dB) is assumed in this study;
- loss due to clutter where one end of the interference path is within man-made clutter (IMT-2020 systems), and the other is the DRS satellite; these losses could be modelled using Rec. ITU-R P.2108 for Earth-space when the terrestrial environment is urban or suburban.

4 Technical analysis

This section aims at providing the coexistence study between European DRS GSO satellite operating at 9°E and IMT-2020 systems (BSs and UEs) on a cumulative effect of interference basis. The aggregate impact is assessed with static approach, i.e. with a given position of the non-GSO satellite to which the DRS satellite is communicating in 25.25-27.27 GHz band. The calculation used in this analysis is based on the following Steps:

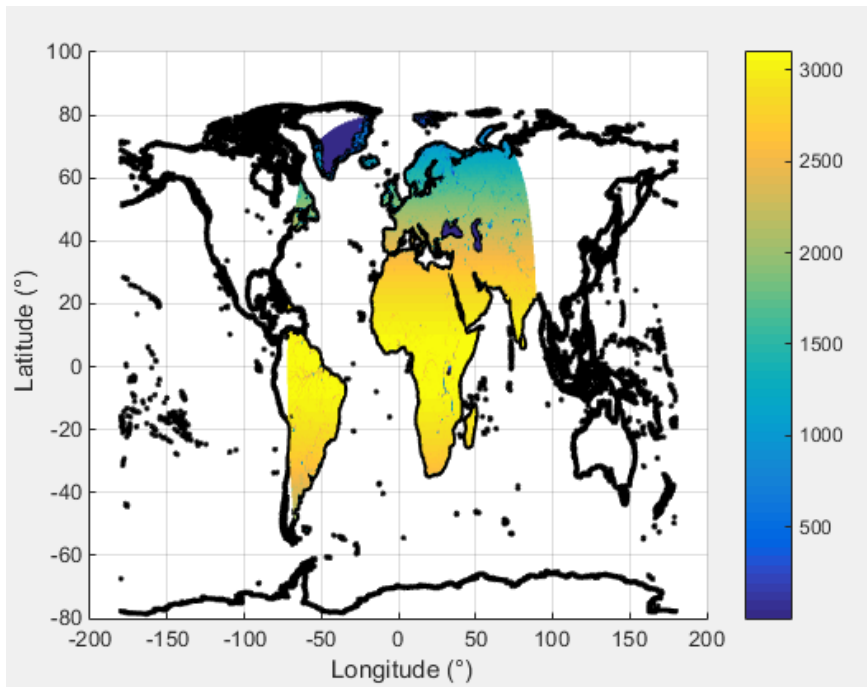
Step 1: Within the DRS satellite visibility area, a land grid map is created with a Step of 0.5° in longitude and 0.5° in latitude, resulting in splitting the map into N_c $0.5^\circ \times 0.5^\circ$ cells; as depicted in Figure 6.

FIGURE 6
Land grid map in the EDRS (9°E) visibility area



Step 2: A grid of N_c elementary surfaces is created in the DRS satellite visibility area. The elementary surface is defined by a Step of 0.5° in longitude and latitude and is expressed in km^2 . It depends on the elementary surface latitude as shown in Figure 7.

FIGURE 7
Elementary surface in km² in the EDRS (9°E) visibility area



Step 3: A grid of the number of BSs and UEs (N_{UE_n} , N_{BS_n}) transmitting simultaneously in an elementary surface n (see Step 2) is created. N_{BS_n} N_{UE_n} are defined as follows:

$$N_{BS_n} = N_{BS_{open\ space}} + N_{BS_{hotspot}} = S_n \times BS_{AF} \times BS_{NLF} \times R_b \times (R_{aSU} \times (D_{BS_{SSU}} + D_{BS_{SU}}) + R_{aU} \times D_{BS_U})$$

$$N_{UE_n} = S_n \times UE_{AF} \times UE_{NLF} \times R_b \times (R_{aSU} \times D_{UE_{SU}} + R_{aU} \times D_{UE_U})$$

with:

n index of Step 2 grid (elementary surface grid map);

BS_{AF} , UE_{AF} BS and UE TDD activity factor (80% and 20%)⁷;

BS_{NLF} , UE_{NLF} BS and UE network loading factor (20% for both)⁸;

S_n elementary surface from Step 2 (km²);

R_a the ratio of hotspot areas to areas of cities/built areas/districts (3% for suburban (R_{aSU}) and 7% for urban (R_{aU}))⁷;

R_b the ratio built areas to total area of region in study (5%)⁷;

$D_{BS_{SSU}}$ BS density in outdoor suburban open space (0 or 1 BS/km²)⁷;

⁷ See Document [5-1/36](#).

⁸ 20% would normally represent a typical/average value for the loading of base stations across a network and therefore can be used for a wide area analysis which is the case in this study (see Document [5-1/36](#)).

D_{BSsu}, D_{UESu} BS and UE density in outdoor suburban hotspot (10 BSs/km^2 and 30 UEs/km^2)⁷;

D_{BSu}, D_{UEU} BS and UE density in the outdoor urban hotspot (30 BSs/km^2 and 100 UEs/km^2)⁷.

FIGURE 8

Number of BSs hotspot simultaneously transmitting in an elementary surface of 0.5° in longitude and latitude

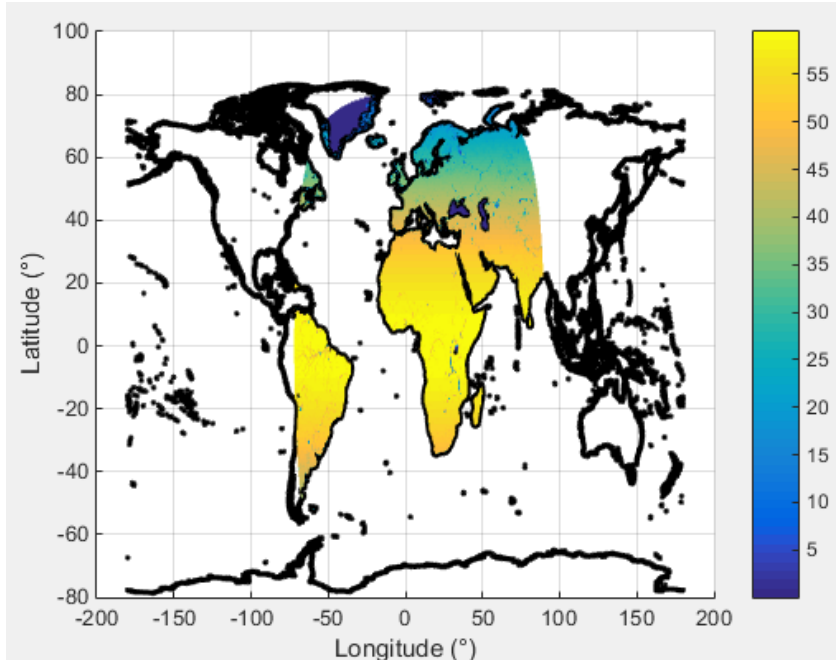


FIGURE 9

Number of BSs open space simultaneously transmitting in an elementary surface 0.5° in longitude and latitude

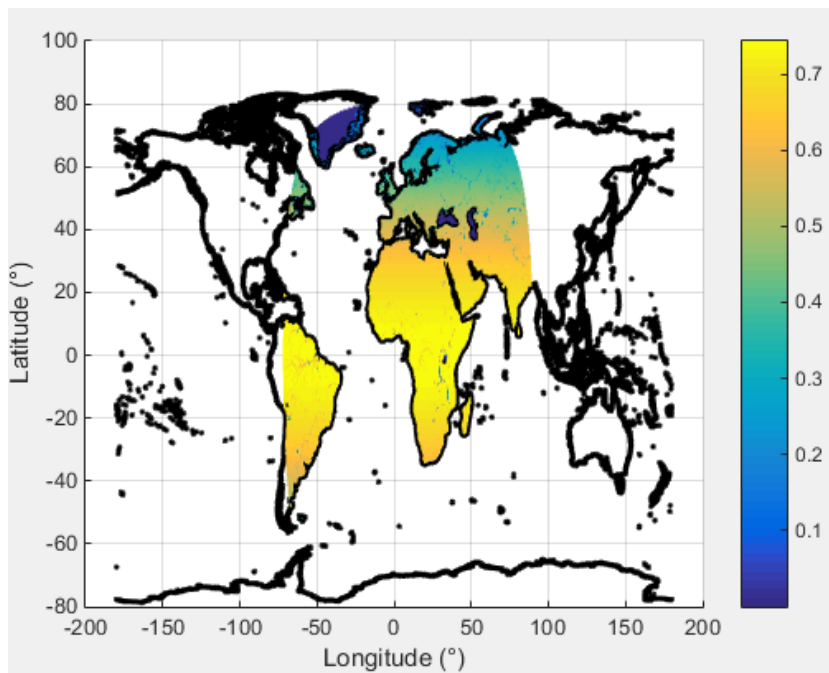
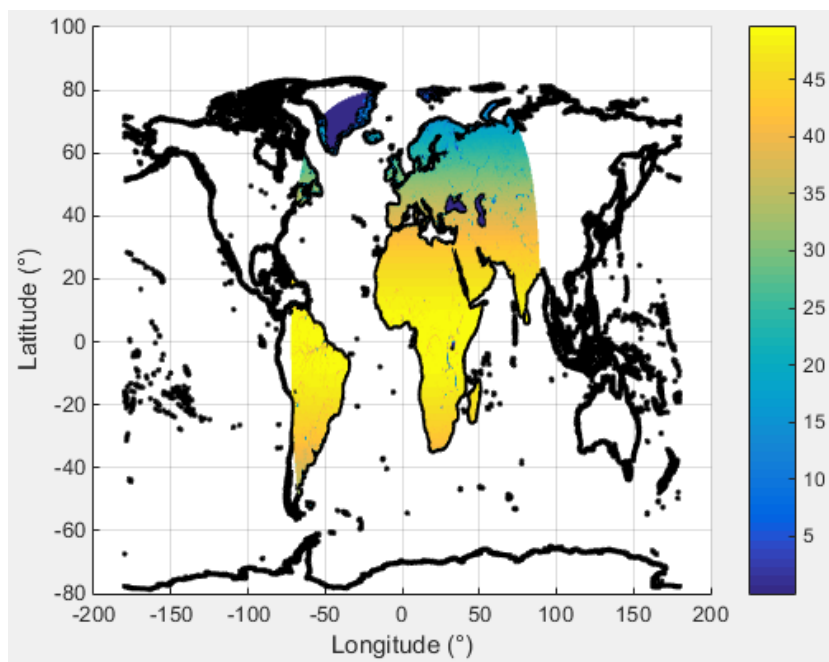


FIGURE 10

Number of UEs simultaneously transmitting in an elementary surface of 0.5° in longitude and latitude



Step 4: the average BS and UE antenna gain are computed as shown in the Annex 1. It is elevation dependent.

FIGURE 11

BS Average antenna gain (at 6 m) towards the European DRS satellite (dBi)

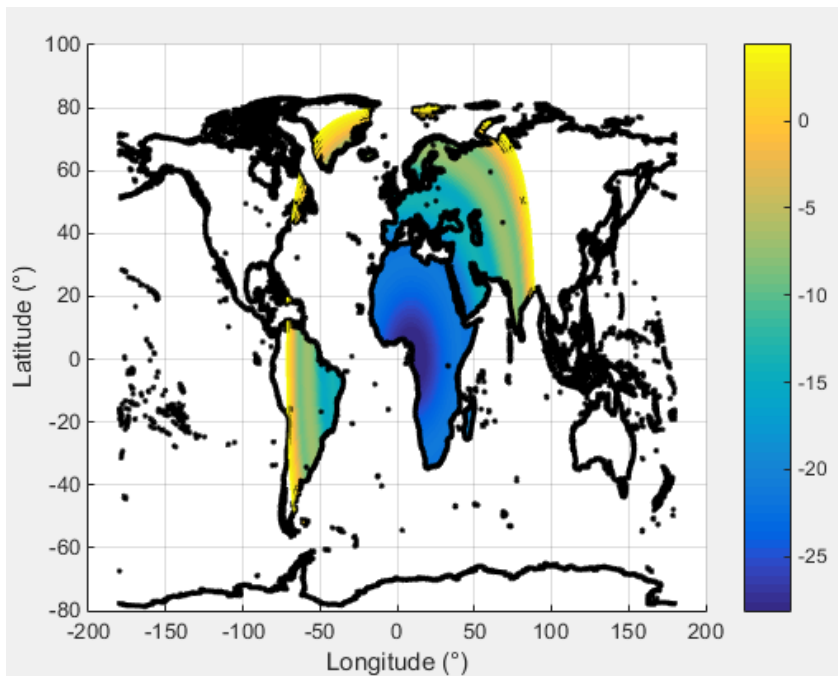


FIGURE 12

BS Average antenna gain (at 15 m) towards the European DRS satellite (dBi)

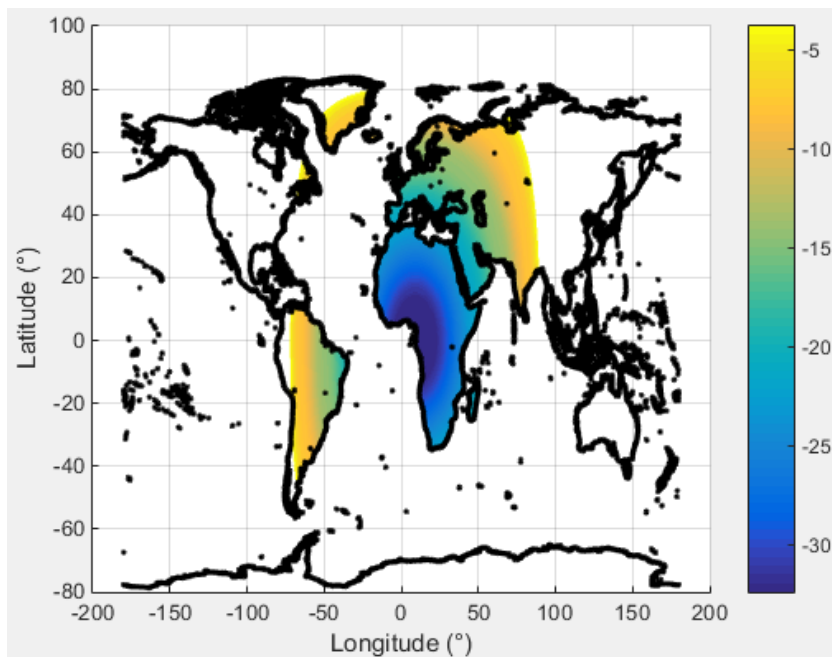
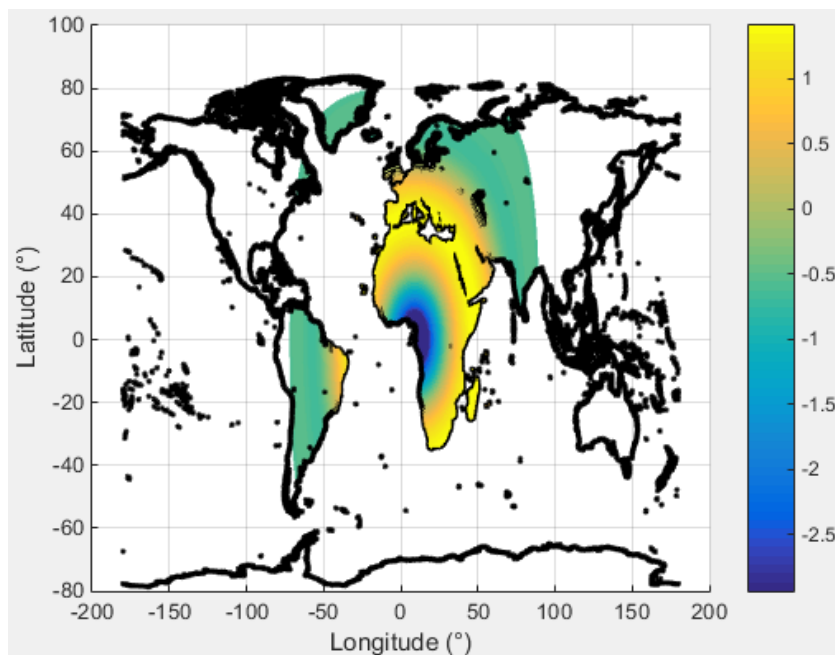


FIGURE 13

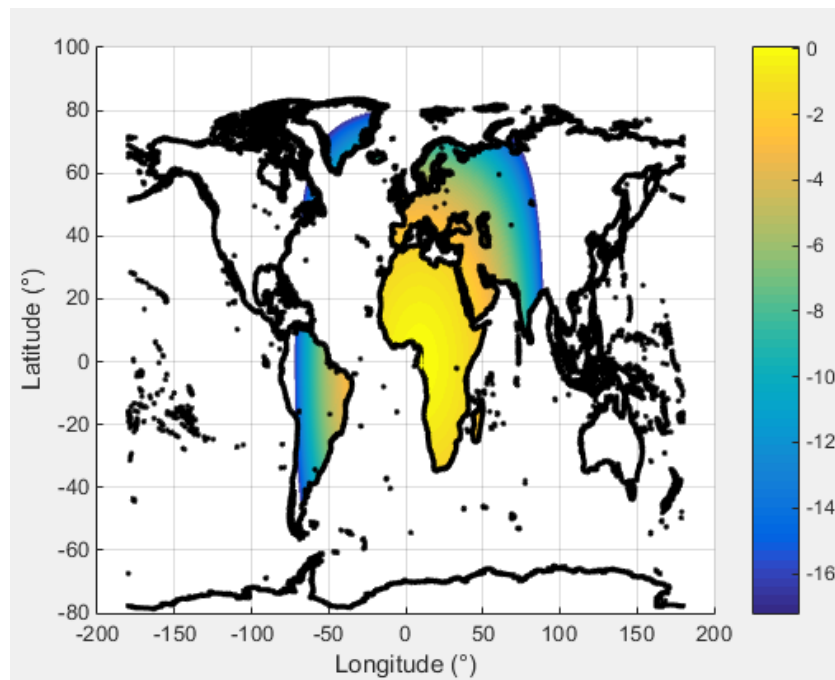
UE Average antenna gain (at 6 m and 15 m⁹) towards the European DRS satellite (dBi)



Step 5: The clutter loss is computed, noting that it is not different from BS (at 6 m) and UEs in Figure 14.

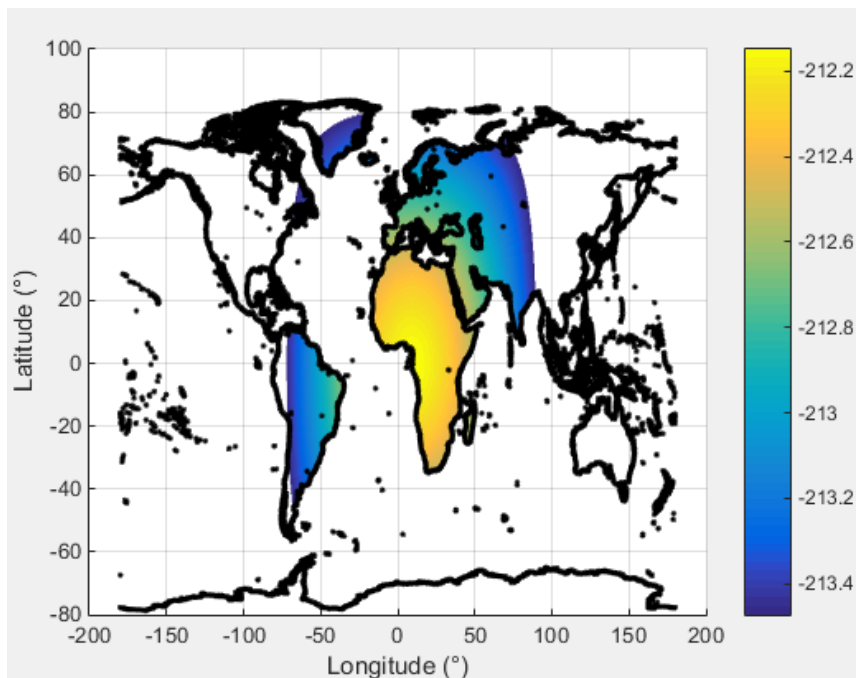
⁹ The results for these 2 cases are very similar (the maximum gap between them is < 0.1 dB).

FIGURE 14
Clutter Loss (dB)



Step 6: The free space loss (FSL) is computed. Figure 15 provides the result for a DRS satellite at 9°E.

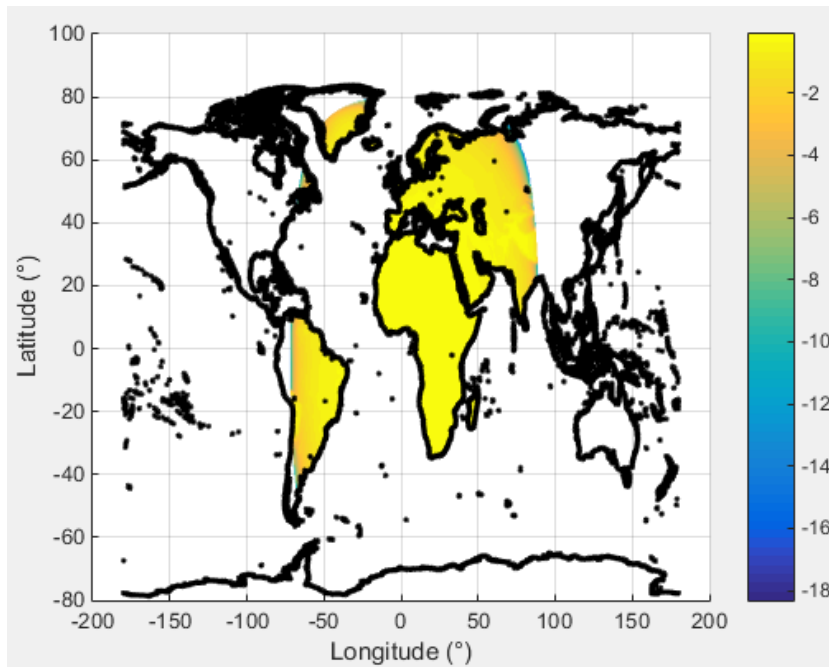
FIGURE 15
Free space loss toward the DRS satellite (in dB)



Step 7: The atmospheric attenuation due to gas is computed using Recommendation ITU-R P.676-11, using the mean annual global reference atmosphere¹⁰. Figure 16 provides the result for a DRS satellite at 9°E.

¹⁰ See Recommendation ITU-R P.835-5, Annex 1, section 1.

FIGURE 16
Attenuation from atmospheric gases (in dB)



Step 8: The aggregate pfd received from each cell of Step 2 grid is computed using the following formulas.

$$\begin{aligned} PFD_{total\ n} &= PFD_{BS\ n} + PFD_{UE\ n} \\ &= 10\log_{10}\left(\sum_{i=1}^{N_{BSn}} 10^{\frac{P_{BS\ i\ n}}{10}} \times 10^{\frac{G_{BS}(etilt, \varphi_{scan}, \theta_{in})}{10}} \times 10^{\frac{L_{gaz\ BS\ in}}{10}} \times \frac{1}{4\pi d_{BS\ in}^2}\right. \\ &\quad \left.+ \sum_{i=1}^{N_{UEn}} 10^{\frac{P_{UE\ i\ n}}{10}} \times 10^{\frac{G_{UE}(etilt, \varphi_{scan}, \theta_{in})}{10}} \times 10^{\frac{L_{gaz\ UE\ in}}{10}} \times \frac{1}{4\pi d_{UE\ in}^2}\right) \end{aligned}$$

with:

i index of the transmitting device (BS or UE) considered;

n index of Step 2 grid (elementary surface grid map) ;

$P_{X\ in}$ the RF power at the input of the antenna of the transmitting device X (BS or UE) in:

$P_{X\ in}$ = Conducted Power per antenna elt (dBm)+10log₁₀(N_{belts})-Array Ohmic Loss

$G_X(etilt_{i\ n}, \varphi_{scan\ n}, \theta_{in})$ transmission antenna gain (dB) of the i^{th} device X (BS or UE) located in cell n forming a beam at $(etilt_{i\ n}, \varphi_{scan\ in})$ in the direction $(\varphi_{in}, \theta_{in})$ of the DRS satellite;

$d_{X\ in}$ distance (m) between the i^{th} device X (BS or UE) located in cell n and the DRS-satellite;

N_{Xn} number of devices X (BS or UE) simultaneously transmitting in cell n (see Figure 8 and Figure 9 for BSs and Figure 10 for UEs);

L_{gazXin} atmospheric attenuation in dB (Rec. ITU-R P.676-11, see Figure 19) between i^{th} device X (BS or UE) located in cell n and the DRS satellite.

- Generally, $L_{Atm Xin}$ and d_{xin} can be considered constant over a specific cell n (of Step 2 grid corresponding to the elementary surface grid). The constant values over an elementary surface cell are denominated respectively L_{gazn} and d_n . without the need for distinguishing the concerned device (UE or BS). Therefore, the above equation can be expressed as follows:

$$PFD_{total\ n} = PFD_{BS\ n} + PFD_{UE\ n} = L_{gaz_n} - 10 \log_{10}(4\pi d_n^2) \\ + 10 \log_{10} \left(\sum_{i=1}^{N_{BSn}} 10^{\frac{P_{BS\ in}}{10}} \times 10^{\frac{G_{BS}(etilt,\varphi_{scan},\theta_{in})}{10}} + \sum_{i=1}^{N_{UEn}} 10^{\frac{P_{UE\ in}}{10}} \times 10^{\frac{G_{UE}(etilt,\varphi_{scan},\theta_{in})}{10}} \right)$$

However, it has to be mentioned that the number of BSs and UEs who are in visibility of the DRS satellite with the same (fixed) elevation θ ($\theta=0..90^\circ$) is high (because of the high amount of $0.5^\circ \times 0.5^\circ$ cells associated to the same (fixed) elevation θ combined with the number of BSs within each of them) based on Figure 5), the integration of PFDn for all (N_c) cells can be performed by considering the average BS antenna gain towards the European DRS satellite when the BS is located in an area which sees the DRS satellite at a specific elevation angle θ_n , denoted $G_{BS\ av}(\theta_n)$ and $G_{UE\ av}(\theta_n)$ respectively for BS and UE. In that case, PFDn is equal to:

$$PFD_{total\ n} = PFD_{BS\ n} + PFD_{UE\ n} \\ = L_{gaz_n}(dB) - 10 \log_{10}(4\pi d_n^2) + 10 \log_{10} \left(10^{\frac{G_{BS\ av}(\theta_n)}{10}} \sum_{i=1}^{N_{BSn}} 10^{\frac{P_{BS\ in}}{10}} + 10^{\frac{G_{UE\ av}(\theta_n)}{10}} \sum_{i=1}^{N_{UEn}} 10^{\frac{P_{UE\ in}}{10}} \right)$$

- For the BS case, P_{in} is constant ($P_n = 25$ dBm). Therefore, the above equation can be expressed as follows:

$$PFD_{total\ n} = PFD_{BS\ n} + PFD_{UE\ n} \\ = L_{gaz_n}(dB) - 10 \log_{10}(4\pi d_n^2) + 10 \log_{10} \left(P_{BS}(mW) \cdot N_{BSn} \cdot 10^{\frac{G_{BS\ av}(\theta_n)}{10}} + 10^{\frac{G_{UE\ av}(\theta_n)}{10}} \sum_{i=1}^{N_{UEn}} 10^{\frac{P_{UE\ in}}{10}} \right)$$

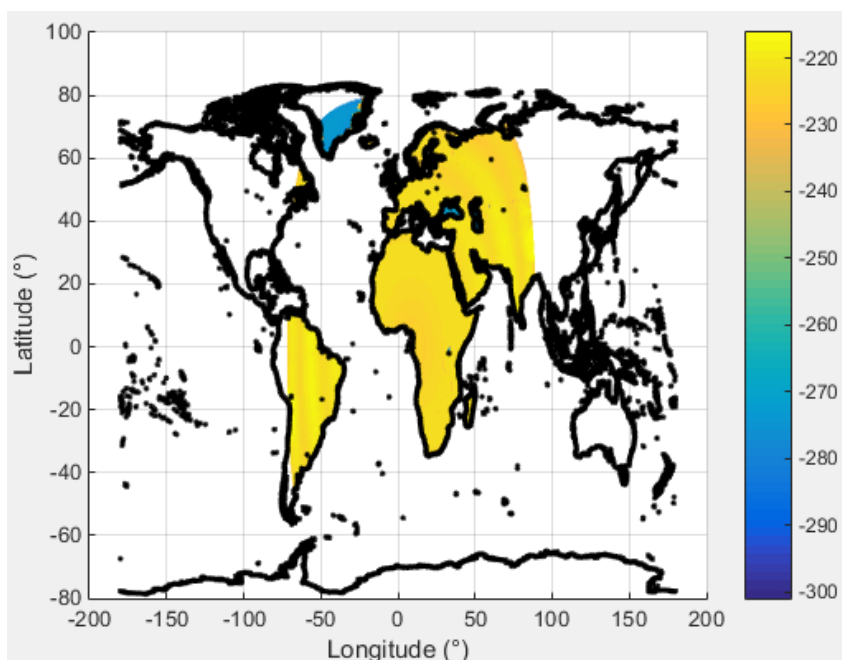
- For the UE case, P_{in} is not constant because of the power control procedure used in relation to the BS. However, similarly to what was applied for the average antenna gain, the average UE conducted power, denoted $P_{UE\ av}$ can be considered in the calculation of the $PFD_{total\ n}$.

$$\boxed{PFD_{total\ n} = L_{gaz_n}(dB) - 10 \log_{10}(4\pi d_n^2) + 10 \log_{10} \left(N_{BSn} P_{BS}(mW) G_{BS\ av}(\theta_n) + N_{UEn} P_{UE\ av}(mW) G_{UE\ av}(\theta_n) \right)}$$

Figure 17 provides the PFD_n map.

FIGURE 17

PFD_n map (dBm/m²/Hz)



Step 9: A grid of EDRS beam pointing direction toward non-GSO satellite is created with a 0.5° Step for the non-GSO satellite longitude and latitude. A typical non-GSO altitude of 700 km is taken for the study. The non-GSO satellite is in visibility from the European DRS satellite (see Figure 19) at 9°E when the distance between the non-GSO satellite and the European DRS satellite is below 44 726 km. Moreover, in order to avoid affecting the DRS-non-GSO satellite radio link with loss due to gaseous atmosphere, an additional 20 km is taken above the surface of the Earth as shown in the following formula and Figure 18:

$$d_{max} = \sqrt{(R_{EDRS})^2 - (R_{Earth} + 20 \text{ km})^2} + \sqrt{(R_{NGSO})^2 - (R_{Earth} + 20 \text{ km})^2} = 44726 \text{ km}$$

FIGURE 18

Non-GSO-DRS satellites link geometry (non-GSO satellite at the limit of the EDRS coverage)

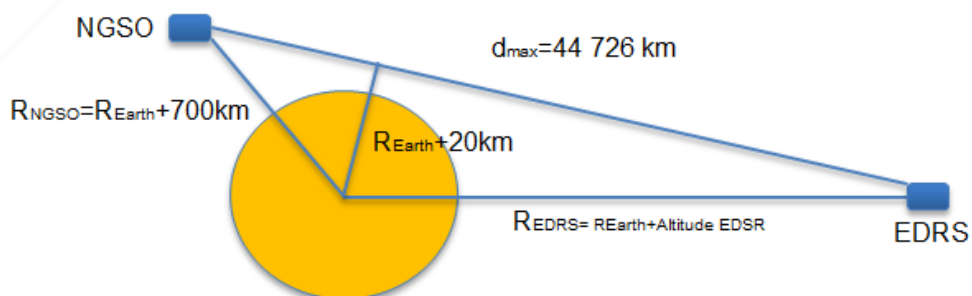
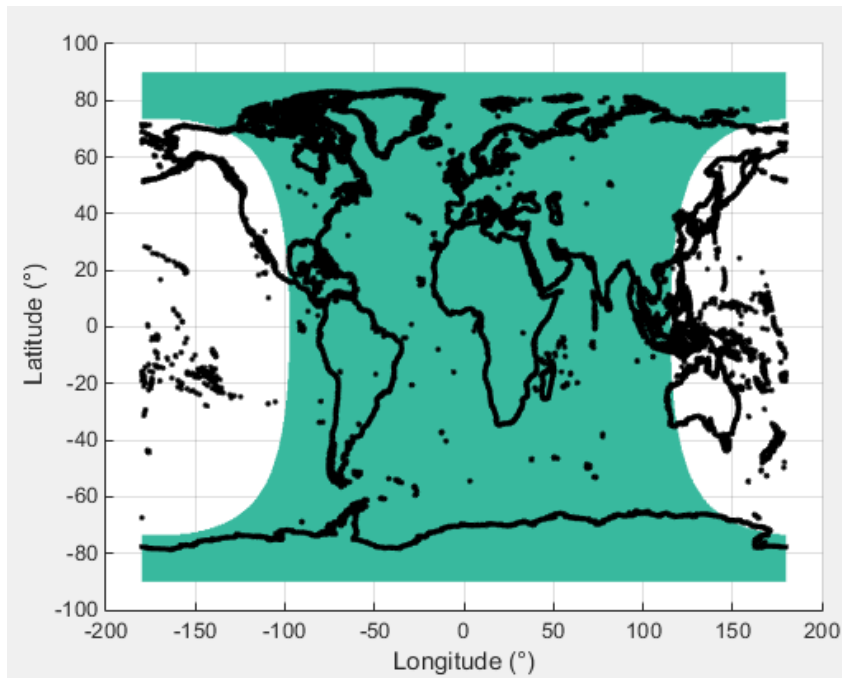


FIGURE 19

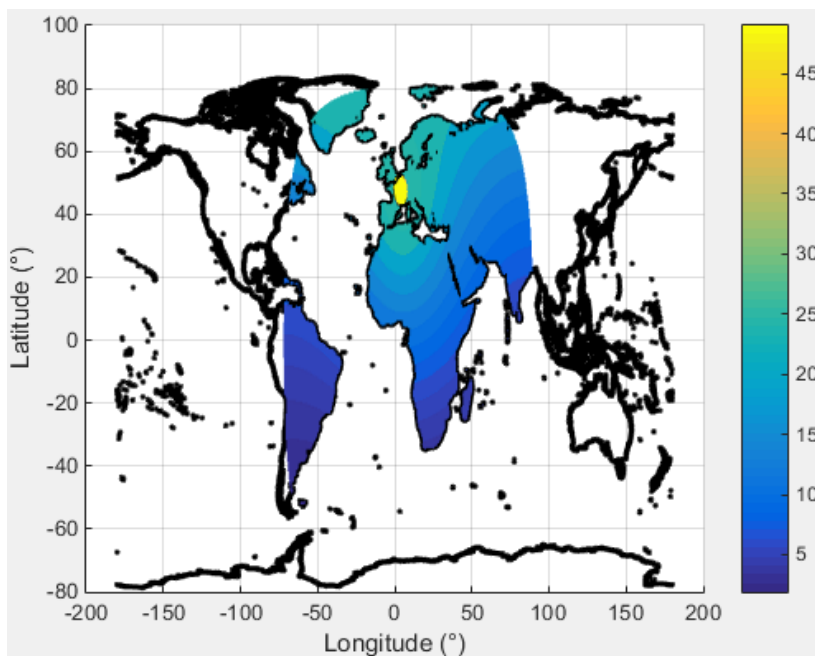
Non-GSO (700 km) visibility area from EDRS (grid $0.5^\circ \times 0.5^\circ$ in longitude and latitude)



Step 10: For a specific EDRS beam pointing direction m (m being the index of Step 6 grid expressed in (latitude, longitude), considering the altitude of the non-GSO satellite as constant), the EDRS beam antenna gain Gr_{mn} towards a specific point n of the Step 2 grid (elementary surface grid) is computed using Recommendation ITU-R S.672-4. Figure 20 below provides an example when the EDRS beam is directed towards a non-GSO satellite at an altitude of 700 km and located at longitude 5°E and latitude 40°N .

FIGURE 20

European DRS antenna gain ($G_{sat,nm}$) towards the Earth (dBi) when pointing towards a non-GSO satellite located at m =(longitude 5°E, latitude 40°N) and altitude 700 km



Step 11: The aggregate interference map is computed (map of I_{nm}). I_{nm} is the aggregate interference in a specific elementary surface cell n when the DRS satellite is pointing towards a specific non-GSO satellite position m within the coverage area defined in Step 9.

$$I_{nm}(Long_{NGSO_m}, Lat_{NGSO_m}, Alt_{NGSO_m}) = PFD_n + Gr_{nm} + L_{polarization}(dB) + 10 \log_{10} \left(\frac{\lambda^2}{4\pi} \right)$$

with:

m the index of the Step 9 grid (European DRS visibility grid);

n the index of Step 2 grid (elementary surface grid);

$L_{polarization}$ the losses due to polarization.

Step 12: The aggregate interference of all BSs and UEs (i.e. for BSs and UEs in all cells) is computed when the DRS satellite is pointing towards the specific direction of Steps 9 and 10 using the following formula. The following result is stored.

$$I_m = \sum_{n=1}^{Nc} (I_{nm}(Long_{NGSO_m}, Lat_{NGSO_m}, Alt_{NGSO_m}))$$

with:

m index EDRS beam pointing direction towards the non-GSO satellite (index of the Step 5 grid);

n index of the cell of Step 1 or 2 grid (land map or elementary surface map);

Nc number of point in the Step 1 or 2 grid;

$Long_{non-GSO_m}$ longitude of the non-GSO satellite;

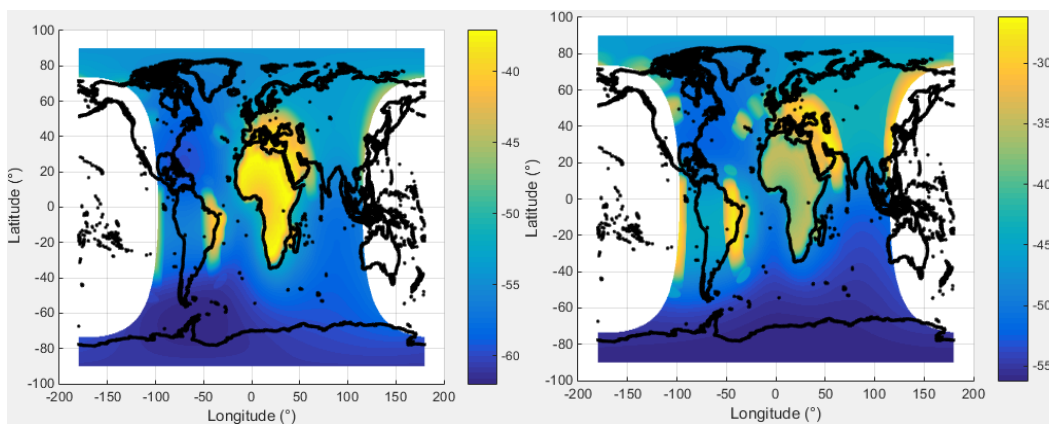
$Lat_{non-GSOm}$ latitude of the non-GSO satellite;

$Alt_{non-GSOm}$ altitude of the non-GSO satellite (a typical non-GSO satellite altitude of 700 km is taken in the study).

Step 13: Redo Steps 10 to 12 for all possible EDRS beam pointing direction (see Step 9). Finally, derive I_{om}/N_o , where N_o depicts the system noise power density. Figure 21 highlights the results (I_{om}/N_o map).

FIGURE 21

Static aggregate I_o/N_o map (dB) due to UEs only (left side) and due to BSs and UEs (right side) when the European DRS satellite is pointing towards a non-GSO satellite located at 700 km altitude

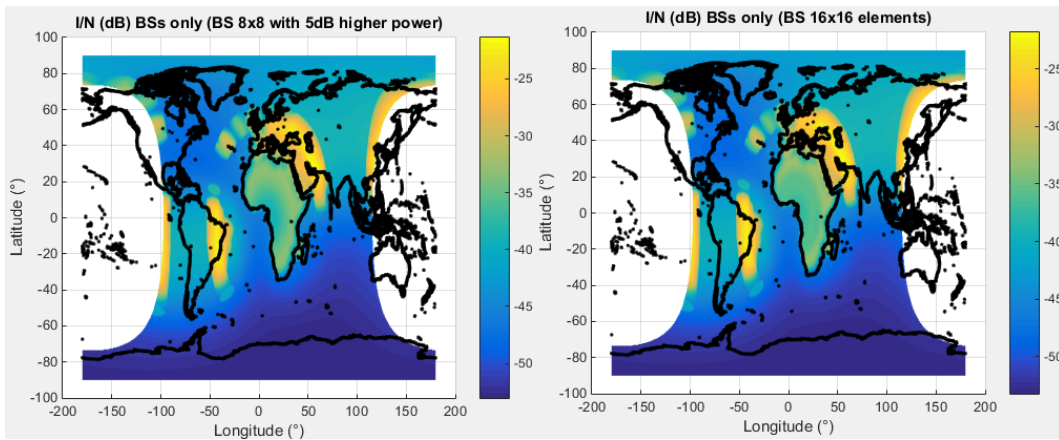


It can be observed that the impact of the UEs ($I_o/N_o \text{ max} = -34.1 \text{ dB}$) is negligible compared to the BSs ($I_o/N_o \text{ max} = -26.4 \text{ dB}$), which explains why the maximum static aggregate I_o/N_o value is achieved at -26.2 dB when both devices are accounted in the cumulative effect (which is more than 16 dB below the protection criterion $I_o/N_o = -10 \text{ dB}$). Moreover, sensitivity analysis provided in Figure 22 indicates that:

- when considering 5 dB higher conducted power for the BSs, the protection criterion is still met with a margin higher than 11 dB (having $I_o/N_o \text{ max} = -21.4 \text{ dB}$ for BSs only);
- when BSs antennas radiate within a 16×16 elements configuration, $I_o/N_o \text{ max} = -21.8 \text{ dB}$ for BSs only.

FIGURE 22

Static aggregate I_o/No map (dB) due to BSs only for different sensitivity analysis



Since the static aggregate study shows that there is never any exceedance of the protection criterion ($I_o/No = -10$ dB) for the case of the European DRS satellite at 9°E, no dynamic sharing study is further required to investigate the coexistence between European DRS and IMT-2020 systems in 25.25-27.5 GHz band.

5 Summary and analysis of the results of studies

This study provides an assessment of compatibility between IMT-2020 systems and the European DRS at 9°E operating in 25.25-27.5 GHz accounting the cumulative effect of both BSs and UEs in-band emissions. It has to be noted that:

- the coexistence analysis addressed all cases of EDRS beam pointing directions of the GSO satellite (at 9°E) to the non-GSO satellite (operating at constant altitude = 700 km);
- the clutter loss assumption was considered for the BSs not located at the roof of the buildings and for all UEs;
- the distribution of the beam pointing antenna, i.e. electrical tilt and phi-scan followed the methodology described in the previous TG 5/1 Chairman's Report;
- the BS and UE deployment assumptions follow the guidance of Document 5-1/36 (provided by WP 5D).

The result shows that the protection criterion ($I_o/No = -10$ dB) of the European DRS satellite (at 9°E) is met with more than 16 dB margin. When considering 5 dB higher conducted power for the BSs or 16x16 elements antenna as sensitivity analysis, the protection criterion is still met with a margin higher than 11 dB.

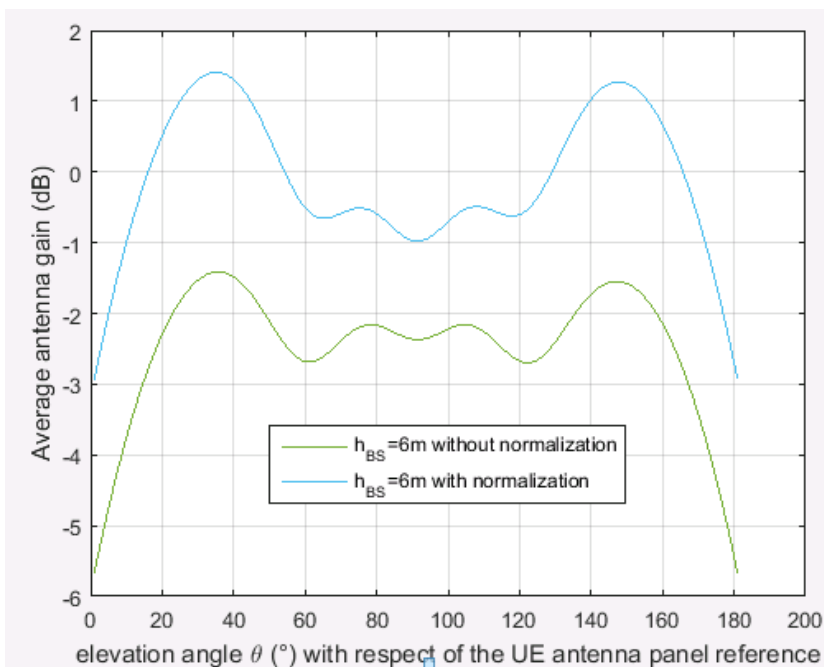
ANNEX 1

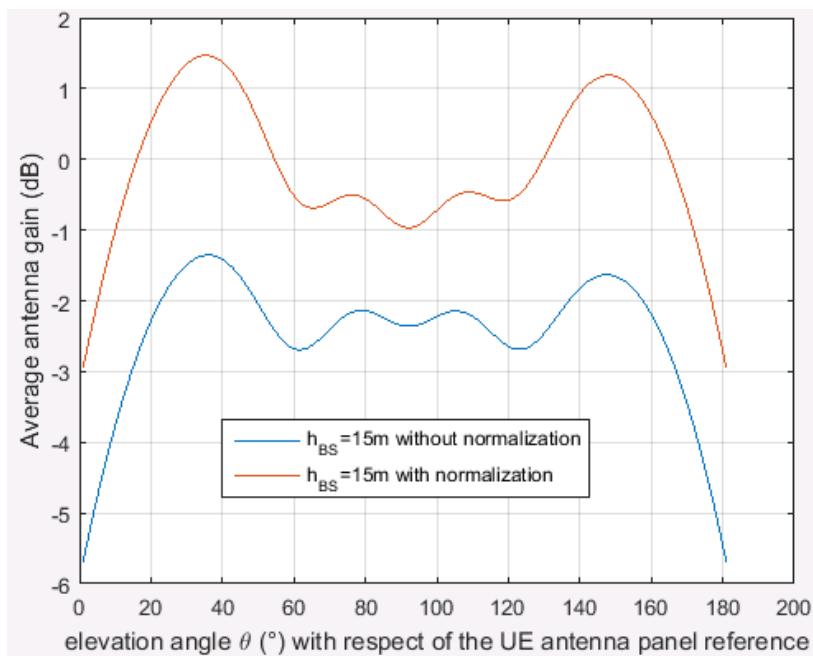
Average antenna gain of IMT-2020 systems

This section provides the behaviour of the average antenna gain as a function of the elevation angle for different configurations: BS and UE as well as the consideration of the normalization factor on the antenna gain calculation.

It is important to note that **the BS and UE average antenna gains as depicted below were calculated relative to the Earth-centred coordinated system**. This means that a rotation of the coordinate system (from Local Coordinate System (LCS) as to be the IMT-2020 antenna system to the Global Coordinate System (GCS) as to be the Earth) was performed in accordance with section 5.1.4 of the 3GPP TS 36.873. This rotation is of the BS mechanical downtilt around y axis (fixed for the BS, variable for the UE).

1 UE case





2 BS case (8×8 elements)

FIGURE 23
Average gain (BS mechanical tilt=10°)

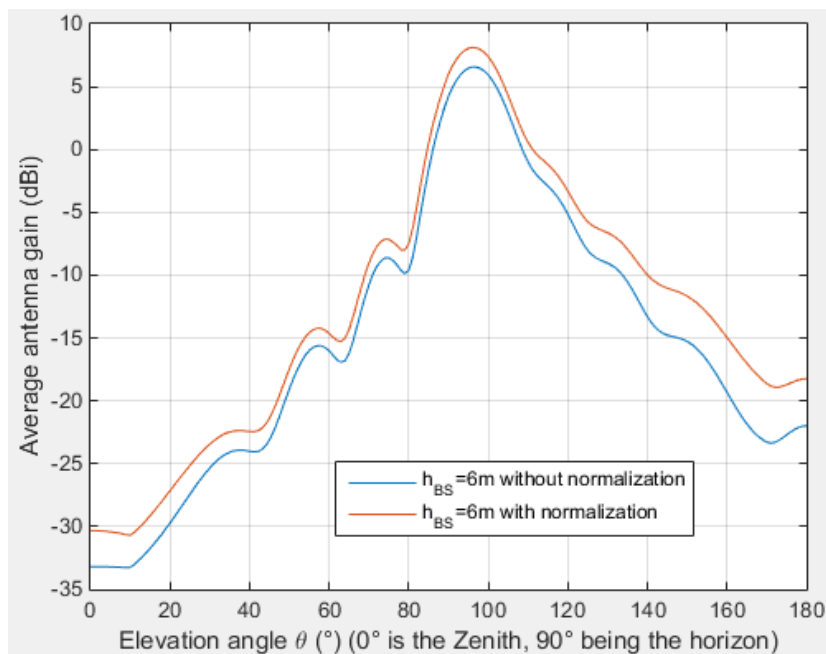
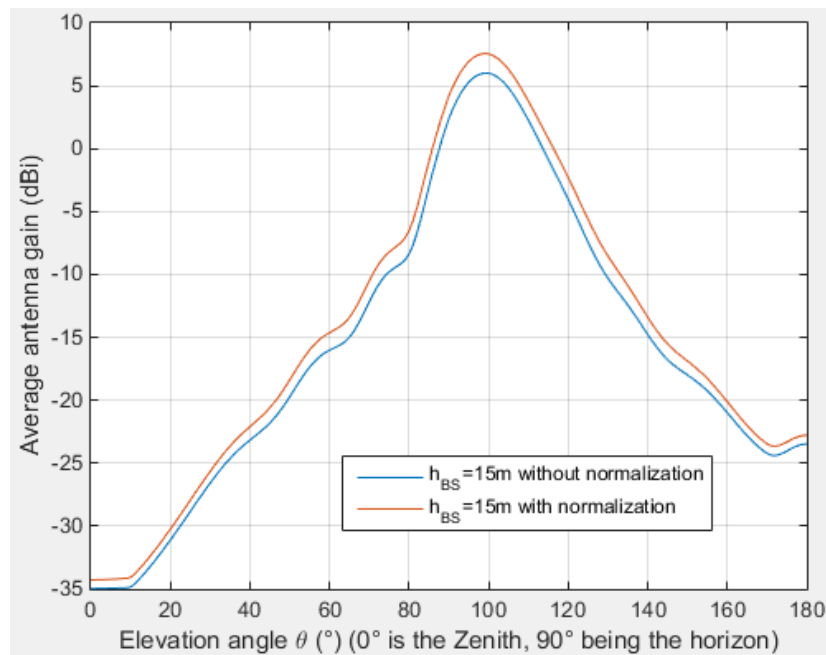


FIGURE 24

Average gain (BS mechanical tilt = 15°)



2 BS case (16×16 elements)

FIGURE 25

Average gain (BS mechanical tilt=10°)

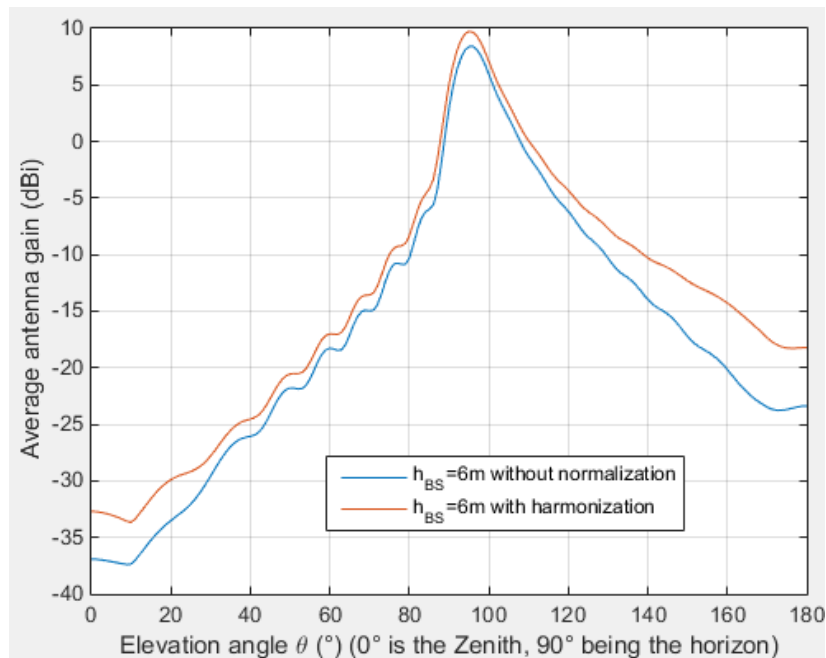


FIGURE 26

Average gain (BS mechanical tilt = 15°)

